Ross scheme, Newton-Raphson iterative methods and time-stepping strategies for solving the mixed-form of Richards' equation

Hassane[1,2] Mamadou Maina F. Z., Ackerer[1,*] P.

[1]Laboratoire d'Hydrologie et de Géochimie de Strasbourg,
Univ. Strasbourg/EOST - CNRS
1 rue Blessig, 67084 Strasbourg,
France

[2]CEA-Laboratoire de Modélisation des Transferts dans l'Environnement,
Bât. 225, F-13108 Saint Paul lez Durance cedex,
France

*Corresponding author: ackerer@unistra.fr

ABSTRACT

1   The solution of the mathematical model for flow in variably saturated porous media described

2   by Richards equation (RE) is subject to heavy numerical difficulties due to its highly non-

3   linear properties and remains very challenging. Two different algorithms are used in this work

4   to solve the mixed-form of RE: the traditional iterative algorithm and a time-adaptive

5   algorithm consisting of changing the time step magnitude within the iteration procedure while

6   the state variable is kept constant. The Ross method is an example of this type of scheme, and

7   we show that it is equivalent to the Newton-Raphson method with a time-adaptive algorithm.

8   Both algorithms are coupled to different time stepping strategies: the standard heuristic

9   approach based on the number of iterations and two strategies based on the time truncation

10 error or on the change of water saturation. Three different test cases are used to evaluate the

11 efficiency of these algorithms.

12 The numerical results highlight the necessity of implementing two types of errors: the

13 iterative convergence error (maximum difference of the state variable between two iterations)

14 and an estimate of the time truncation errors. The algorithms using these two types of errors

15 together were found to be the most efficient when highly accurate results are required.

16

17 **Key words**: Unsaturated flow, Newton-Raphson, Time stepping

Hydrology and
Earth System
Sciences

Open Access

Discussions

EGU

1. Introduction

18

19   Water movement in soils is one of the key processes in the water cycle since it contributes to

20   the renewal of groundwater resources through recharge, to vegetation growth through

21   transpiration, to soil fertility through salinization/alteration and to atmospheric humidity

22   through evaporation and transpiration. Water movement is usually modeled using the

23   Richards equation (Richards, 1931), which is now commonly adopted for many studies in soil

24   science and/or hydrology, including the use of physically based hydrological models applied

25   to large-scale catchments and for long time simulations (e.g., for climate change studies).

26   However, this equation is highly nonlinear and despite numerous efforts over the last 40

27   years, its numerical solution requires much computational time.

28   Assuming a rigid solid matrix, the Richards equation (RE) is given by,

29
$$
\begin{cases}
\dfrac{\partial \theta}{\partial t} + S_w s_0 \dfrac{\partial \psi}{\partial t} + \nabla \cdot \mathbf{q} = f \\
\mathbf{q} = -k_r(\psi)\mathbf{K}\left[\nabla \psi + \nabla z\right]
\end{cases}
\tag{1}
$$

30   where θ is the volumetric water content [L^3/L^3], S_w is the water saturation [-], s_0 is the specific

31   storage coefficient [L^{-1}], ψ is the pressure head [L], $\mathbf{q}$ is the water flux based on the extended

32   Darcy's law [L/T], t is the time [T], z is the vertical coordinate (positive upward) [L], f is the

33   sink/source term [T^{-1}], $\mathbf{K}$ is the saturated hydraulic conductivity tensor [L/T] and $k_r(\psi)$ is the

34   relative hydraulic conductivity [-]. The model includes initial and boundary conditions of the

35   Dirichlet (prescribed pressure head) or Neumann (prescribed flux) type.

36   Equation (1) is also called the mixed form of RE. Two alternative formulations exist for RE.

37   The pressure form is defined by:

38
$$
\begin{cases}
\left[C(\psi) + S_w s_0\right]\dfrac{\partial \psi}{\partial t} + \nabla \cdot \mathbf{q} = f \\
\mathbf{q} = -k_r(\psi)\mathbf{K}\left[\nabla \psi + \nabla z\right]
\end{cases}
\tag{2}
$$

39   where $C(\psi) = \dfrac{\partial \theta}{\partial \psi}$ is the specific moisture capacity [L^{-1}], and the soil moisture form that is

40   restricted to unsaturated conditions is defined by:

$$
\begin{cases}
\dfrac{\partial \theta}{\partial t} + \nabla \cdot \mathbf{q} = f \\
\mathbf{q} = -\left(\mathbf{D}(\theta)\nabla\theta + k_r(\theta)\mathbf{K}\nabla z \right)
\end{cases}
\tag{3}
$$

42   where $\mathbf{D}(\theta) = k_r(\theta)\mathbf{K}\dfrac{d\psi}{d\theta}$ is the pore water diffusivity [L^2/T].

43   Constitutive relations are required to solve RE. For the pressure-water content relationship,

44   the most common model is the Van Genuchten model (van Genuchten, 1980):

$$
S_w(\psi) = \frac{\theta(\psi) - \theta_r}{\theta_s - \theta_r} =
\begin{cases}
\left(1 + \left| \alpha\psi \right|^\eta \right)^{-m} & \psi < 0 \\
1 & \psi \geq 0
\end{cases}
\tag{4}
$$

46   where $m = 1 - 1/\eta$, S_w is the effective saturation, θ_r and θ_s are the residual and saturated

47   volumetric water content respectively, α and η are experimentally estimated coefficients.

48   This model is usually associated with Mualem model (Mualem, 1976) for the relative

49   permeability of the aqueous phase:

$$
k_r(S_w) =
\begin{cases}
S_w^{1/2}\left[1 - \left(1 - S_w^{1/m} \right)^m \right]^2 & \psi < 0 \\
1.0 & \psi \geq 0
\end{cases}
\tag{5}
$$

51   A summary of the most popular relations can be found in Belfort et al. (2013).

52   Due to the strong heterogeneities of the unsaturated zone and nonlinearities in the constitutive

53   relations (Eq. (4) and (5)), analytical solution of RE does not exist except in special cases

54   (Celia et al., 1990; van Dam and Feddes, 2000). Therefore, numerical methods such as finite

55   difference (Feddes et al., 1988; Romano et al., 1998; van Dam and Feddes, 2000), finite

Hydrology and
Earth System
Sciences
Discussions

Open Access

EGU

56   element (Gottardi and Venutelli, 2001), and mixed finite element (Bause and Knabner, 2004;

57   Bergamaschi and Putti, 1999; Fahs et al., 2009; Farthing et al., 2003) are used to solve RE.

58   Iterative methods based on the Picard (fixed point) or Newton-Raphson approach (Lehmann

59   and Ackerer, 1998; Paniconi and Putti, 1994) are the most popular techniques for solving this

60   highly nonlinear equation. Alternative iterative methods are based on transform formulations

61   (Crevoisier et al., 2009; Ross and Bristow, 1990; Williams et al., 2000; Zha et al., 2013) or

62   the method of lines (Fahs et al., 2009; Matthews et al., 2004; Miller et al., 1998; Tocci et al.,

63   1997). Additionally, very few non-iterative schemes have been developed (Kavetski and

64   Binning, 2004, 2002a; Paniconi et al., 1991).

65

66   Despite the many existing numerical methods, solution of the RE is still a challenging

67   research topic with many remaining questions about reduction of the computational time,

68   treatment of nonlinearities, and improvement of the accuracy of these methods for difficult

69   problems such as infiltration in very dry soils (Diersch and Perrochet, 1999; Forsyth et al.,

70   1995; R. G. Hills, 1989).

71   In this study, we analyzed the performance of different algorithms based on the Newton-

72   Raphson method since the classical Picard scheme has been found less efficient (Lehmann

73   and Ackerer, 1998). Applied to the soil moisture form of the RE equation, we demonstrate

74   that the recently developed Ross method (Ross, 2003; Crevoisier et al., 2009; Zha et al., 2013)

75   is equivalent to Newton-Raphson method (section 2). A detailed presentation of the Newton-

76   Raphson method applied to the mixed form or RE is given in section 3. The standard Newton-

77   Raphson algorithm is based on the computation of the corresponding matrices in an iterative

78   way by updating the parameters until convergence. An alternative algorithm has been

79   suggested more recently where the parameters are kept unchanged within one time step and

Hydrology and
Earth System
Sciences

Discussions

Open Access

EGU

80   the time step is adapted to reach convergence. This algorithm has been applied to the

81   pressure-based form of RE by Kavetski and Binning (2002a) and to the soil moisture form by

82   Crevoisier et al. (2009), Ross (2003), Zha et al. (2013). Although this algorithm is called "non

83   iterative" because the parameters are not updated during the calculation, iterations may be

84   necessary to adapt the magnitude of the time step. Therefore, in the following, we will refer to

85   the usual algorithm as "iterative" and to the alternative algorithm as "time-adaptive". To our

86   knowledge, this alternative algorithm has never been applied to the mixed form of RE.

87   Section 4 is dedicated to both algorithms and to the time stepping strategy used for solving

88   RE. Finally, in section 5, the numerical accuracy and robustness of the algorithms applied to

89   the mixed-form of RE are evaluated using three different test cases.

90

91   **2. The Ross method and the Newton-Raphson method**

92   The moisture-based formulation is applicable in unsaturated conditions only and is prone to

93   numerical difficulties in the case of heterogeneous soils, explaining the reduced attention

94   directed to this formulation. However, discontinuous water content can be handled by adapted

95   schemes and moisture-based formulation appears to be very accurate for initially dry

96   conditions (Zha et al., 2013, 2015).

97   Ross (2003) suggested a non-iterative formulation that has been recently extended to different

98   soil conditions (Crevoisier et al., 2009; Varado et al., 2006a) and to two and three dimensions

99   (Zha et al., 2013).

100   In its initial one-dimensional finite-volume formulation and for a volume (cell) i, the Ross

101   method (Ross, 2003) is based on the following set of equations:

102
$$\frac{\Delta z}{\Delta t}\left(\theta_i^{n+1} - \theta_i^n\right) = \frac{\Delta z}{\Delta t}\left(\theta_{s,i} - \theta_{r,i}\right)\left(S_i^{n+1} - S_i^n\right) = q_-^\sigma - q_+^\sigma \qquad (6)$$

103   with:

104
$$\begin{cases} q_+^\sigma = q_+^n + \sigma\left[\left(\frac{\partial q_i^n}{\partial S_i^n}\right)\left(S_i^{n+1} - S_i^n\right) + \left(\frac{\partial q_i^n}{\partial S_{i+1}^n}\right)\left(S_{i+1}^{n+1} - S_{i+1}^n\right)\right] \\ q_-^\sigma = q_-^n + \sigma\left[\left(\frac{\partial q_i^n}{\partial S_i^n}\right)\left(S_i^{n+1} - S_i^n\right) + \left(\frac{\partial q_i^n}{\partial S_{i-1}^n}\right)\left(S_{i-1}^{n+1} - S_{i-1}^n\right)\right] \end{cases} \qquad (7)$$

Hydrology and
Earth System
Sciences

Discussions

105   where S_i^{n+1} is the water saturation at cell/node i at time $(n+1)$, q_-^{σ} (resp. q_+^{σ}) is the water flux

106   between cell i and $(i\text{-}1)$ (resp. $i+1$) at time $t = t^n + \sigma\,\Delta t$, $\sigma \in [0,1]$ and Δz is the size of the

107   cell i. $\theta_{s,i}$ is the saturated water content and $\theta_{r,i}$ is the residual water content. For simplicity,

108   we assume here that all cells are of the same size.

109   The previous mass balance equation (6) leads to the following equation for cell i:

110
$$-\left(\frac{\partial q_-^n}{\partial S_{i-1}^n}\right)\left(S_{i-1}^{n+1} - S_{i-1}^n\right) + \left[\frac{\Delta z}{\sigma\Delta t}\left(\theta_{s,i} - \theta_{r,i}\right) - \left(\left(\frac{\partial q_-^n}{\partial S_i^n}\right) - \left(\frac{\partial q_+^n}{\partial S_i^n}\right)\right)\right]\left(S_i^{n+1} - S_i^n\right)$$
$$+\left(\frac{\partial q_+^n}{\partial S_{i+1}^n}\right)\left(S_{i+1}^{n+1} - S_{i+1}^n\right) = q_-^n - q_+^n \tag{8}$$

111

112   The Newton-Raphson method was initially developed as a root-finding algorithm of an

113   arbitrary equation that has been generalized for solving a system of non-linear equations.

114   Applied to the soil moisture form of the RE and using an implicit scheme, the NR consists in

115   defining a residual based on the mass balance equation (Eq. (6)) at iteration k for time step

116   $n+1$ and for cell i written as:

117
$$R_i^{n+1,k} = \frac{\Delta z}{\Delta t}\left(\theta_{s,i} - \theta_{r,i}\right)\left(S_i^{n+1,k} - S_i^n\right) + q_+^{n+1,k} - q_-^{n+1,k} \tag{9}$$

118   where $R_i^{n+1,k}$ is called the residual.

119   The NR consists in computing the solution at iteration $k+1$ by estimating the residual of the

120   next iteration $R_i^{n+1,k+1}$ using a first order Taylor development and setting it equal to zero as:

121
$$\frac{R_i^{n+1,k}}{\partial S^{n+1,k}}\left(S_i^{n+1,k+1} - S_i^{n+1,k}\right) + R_i^{n+1,k} = 0 \tag{10}$$

122

123   The derivatives of this residual are:

124
$$\begin{cases} \dfrac{\partial R_i^{n+1,k}}{\partial S_{i-1}^{n+1,k}} = -\dfrac{\partial q_-^{n+1,k}}{\partial S_{i-1}^{n+1,k}} \\[2mm] \dfrac{\partial R_i^{n+1,k}}{\partial S_i^{n+1,k}} = \dfrac{\Delta z}{\Delta t}\left(\theta_{s,i} - \theta_{r,i}\right) + \dfrac{\partial q_+^{n+1,k}}{\partial S_i^{n+1,k}} - \dfrac{\partial q_-^{n+1,k}}{\partial S_i^{n+1,k}} \\[2mm] \dfrac{\partial R_i^{n+1,k}}{\partial S_{i+1}^{n+1,k}} = \dfrac{\partial q_+^{n+1,k}}{\partial S_{i+1}^{n+1,k}} \end{cases} \tag{11}$$

7

Hydrology and
Earth System
Sciences
Discussions

125

126 which leads to the following set of linear equations:

127
$$-\frac{\partial q_-^{n+1,k}}{\partial S_{i-1}^{n+1,k}}\left(S_{i-1}^{n+1,k+1}-S_{i-1}^{n+1,k}\right)+\left[\frac{\Delta z}{\Delta t}\left(\theta_{s,i}-\theta_{r,i}\right)+\frac{\partial q_+^{n+1,k}}{\partial S_i^{n+1,k}}-\frac{\partial q_-^{n+1,k}}{\partial S_i^{n+1,k}}\right]\left(S_i^{n+1,k+1}-S_i^{n+1,k}\right)$$
$$+\frac{\partial q_+^{n+1,k}}{\partial S_{i+1}^{n+1,k}}\left(S_{i+1}^{n+1,k+1}-S_{i+1}^{n+1,k}\right)=\frac{\Delta z}{\Delta t}\left(\theta_{s,i}-\theta_{r,i}\right)\left(S_i^{n+1,k}-S_i^n\right)+q_+^{n+1,k}-q_-^{n+1,k}$$
(12)

128

129 For the first iteration, we have $S_i^{n+1,k+1}=S_i^{n+1}$ and $S_i^{n+1,k}=S_i^n$, and therefore :

130
$$-\frac{\partial q_-^n}{\partial S_{i-1}^n}\left(S_{i-1}^{n+1}-S_{i-1}^n\right)+\left[\frac{\Delta z}{\Delta t}\left(\theta_{s,i}-\theta_{r,i}\right)+\frac{\partial q_+^n}{\partial S_i^n}-\frac{\partial q_-^n}{\partial S_i^n}\right]\left(S_i^{n+1}-S_i^n\right)$$
$$+\frac{\partial q_+^n}{\partial S_{i+1}^n}\left(S_{i+1}^{n+1}-S_{i+1}^n\right)=q_+^{n,k}-q_-^{n,k}$$
(13)

131

132 Whatever the formulation of the fluxes q (as a function of the pressure or the water content,

133 expressed by Kirchhoff transform as in Ross (2003) or not), the implicit Ross method (eq. (8)

134 with $\sigma=1$)) is equivalent to the first iteration of the Newton-Raphson method (eq. (13)).

135

136 **3. Newton Raphson method for the mixed form Richards' equation**

137 Because the pressure-based formulation does not ensure mass conservation - except for the

138 approximation provided by Rathfelder and Abriola (1994) - and due to the limitations of the

139 moisture-based formulation (see previous section), the mixed formulation has been widely

140 used since the work of Celia et al. (1990).

141 The mixed form of the Richards equation given by equation (1) is rewritten as:

142
$$\frac{\partial \theta}{\partial t}+S_w s_0\frac{\partial \psi}{\partial t}=\nabla\cdot k_r(\psi)\mathbf{K}\left[\nabla\psi+\nabla z\right]+f$$
(14)

143 and is discretized by:

144
$$\mathbf{A}^{n+1,k}\mathbf{\psi}^{n+1,k+1}+\mathbf{B}^{n+1,k}\frac{\mathbf{\psi}^{n+1,k+1}-\mathbf{\psi}^n}{\Delta t^{n+1}}+\mathbf{E}\frac{\mathbf{\theta}^{n+1,k+1}-\mathbf{\theta}^n}{\Delta t^{n+1}}=\mathbf{F}^{n+1,k}$$
(15)

Hydrology and
Earth System
Sciences

Open Access

Discussions

EGU

145   where **A** is the discretized form of the divergence term, **B** and **E** are the discretized forms of

146   the storage terms and **F** is the discretized form of the sink/source term and the boundary

147   conditions, n is the time step and k the iteration counter. Δt^{n+1} is the time step magnitude

148   defined by $\Delta t^{n+1} = t^{n+1} - t^n$. Matrices **A, B, E** and vector **F** depend on the numerical scheme

149   used for the spatial discretization. The implicit scheme is applied for the spatial discretization.

150   For the Newton-Raphson method, the residual is defined now by:

151
$$\mathbf{R}(\boldsymbol{\psi}^{n+1,k}) = \mathbf{A}^{n+1,k}\boldsymbol{\psi}^{n+1,k} + \mathbf{B}^{n+1,k}\frac{\boldsymbol{\psi}^{n+1,k} - \boldsymbol{\psi}^n}{\Delta t^{n+1}} + \mathbf{E}\frac{\boldsymbol{\theta}^{n+1,k} - \boldsymbol{\theta}^n}{\Delta t^{n+1}} - \mathbf{F}^{n+1,k} \tag{16}$$

152   and its derivatives are:

153
$$\mathbf{R}'(\boldsymbol{\psi}^{n+1,k}) = \mathbf{A}^{n+1,k} + \frac{\partial \mathbf{A}^{n+1,k}}{\partial \boldsymbol{\psi}^{n+1,k}}\boldsymbol{\psi}^{n+1,k} + \frac{\mathbf{B}^{n+1,k}}{\Delta t^{n+1}} + \frac{\partial \mathbf{B}^{n+1,k}}{\partial \boldsymbol{\psi}^{n+1,k}}\frac{\boldsymbol{\psi}^{n+1,k} - \boldsymbol{\psi}^n}{\Delta t^{n+1}}$$
$$+ \frac{\mathbf{E}}{\Delta t^{n+1}}\frac{\partial \boldsymbol{\theta}^{n+1,k}}{\partial \boldsymbol{\psi}^{n+1,k}} - \frac{\partial \mathbf{F}^{n+1,k}}{\partial \boldsymbol{\psi}^{n+1,k}} \tag{17}$$

154   Looking for $\boldsymbol{\psi}^{n+1,k+1}$ such as $\mathbf{R}(\boldsymbol{\psi}^{n+1,k+1}) = 0$, the system to solve is similar to Eq. (10):

155
$$\mathbf{R}'(\boldsymbol{\psi}^{n+1,k})\Delta\boldsymbol{\psi}^{n+1,k+1} = -\mathbf{R}(\boldsymbol{\psi}^{n+1,k}) \tag{18}$$

156   with $\Delta\boldsymbol{\psi}^{n+1,k+1} = \boldsymbol{\psi}^{n+1,k+1} - \boldsymbol{\psi}^{n+1,k}$.

157

158   The NR formulation is also used for the non-iterative scheme by applying only one NR step

159   per time step, with $\boldsymbol{\psi}^{n+1} = \boldsymbol{\psi}^{n+1,1}$ where $\boldsymbol{\psi}^{n+1,0} = \boldsymbol{\psi}^n$ (Paniconi et al., 1991; Zha et al., 2015).

160

161   **4. Algorithms and time stepping strategy**

162   The usual algorithm used to solve RE consists in defining a time step that remains constant

163   and to iteratively compute the parameters and variables in the following way:

164   ***For a given time step n***

165   - Define the time step length Δt^{n+1} depending on the time stepping strategy.

9

166   -   Initialization of the iterative process by setting $\mathbf{\psi}^{n+1,1} = \mathbf{\psi}^n$.

167   *do k=1, maxit*

168   1. Computation of the variable $\mathbf{\theta}^{n+1,k}$, the parameter $\mathbf{K}^{n+1,k}$ and their derivatives

169        $\dfrac{d\mathbf{\theta}^{n+1,k}}{d\mathbf{\psi}^{n+1,k}}, \dfrac{\partial\mathbf{K}^{n+1,k}}{\partial\mathbf{\psi}^{n+1,k}}$ using $\mathbf{\psi}^{n+1,k}$.

170   2. Computation of the system matrix $\mathbf{R}\,'$ and the residual $\mathbf{R}$.

171   3. Computation of the system solution $\mathbf{\psi}^{n+1,k+1}$.

172   4. Check convergence. If convergence is achieved, exit.

173   *enddo*

174   **Next time step**

175   where *k* is the iteration counter and *maxit* the maximum number of iterations.

176

177   The time-adaptive algorithm consists of keeping the pressure head constant and changing the

178   time step length. The algorithm is described by the following:

179

180   **For a given time step n**

181   -   Computation of the variable $\mathbf{\theta}^n$, the parameter $\mathbf{K}^n$ and their derivatives $\dfrac{d\mathbf{\theta}^n}{d\mathbf{\psi}^n}, \dfrac{\partial\mathbf{K}^n}{\partial\mathbf{\psi}^n}$

182   using $\mathbf{\psi}^n$.

183   *do k=1, maxit*

184   1. Define a time step $\Delta t^{n+1,k}$ depending on the time stepping strategy.

185   2. Computation of the system matrix $\mathbf{R}\,'$ and the residual $\mathbf{R}$.

186   3. Computation of the system solution $\mathbf{\psi}^{n+1,k+1}$.

187   4. Check convergence. If convergence is achieved, exit.

188   *enddo*

189   **Next time step**

190

191   The main advantage of the alternative algorithm is its avoidance of the computation of the

192   variable $\mathbf{\theta}$, the parameter $\mathbf{K}$ and their derivatives $\dfrac{d\mathbf{\theta}}{d\mathbf{\psi}}$ and $\dfrac{\partial\mathbf{K}}{\partial\mathbf{\psi}}$ during the iterations. Due to

Hydrology and
Earth System
Sciences
Discussions

Open Access

EGU

193   the highly nonlinear relations between θ, $\mathbf{K}$, $\dfrac{d\theta}{d\psi}$, $\dfrac{\partial \mathbf{K}}{\partial \psi}$ and the pressure, this computation

194   may require significant CPU time.

195

196   The most popular time step management during the simulation is that of the heuristic type

197   (Miller et al., 2006). The time step Δt^{n+1} is computed depending on Δt^n and the number of

198   iterations k necessary to reach convergence in the following way:

199
$$\begin{cases} if \quad k \leq m_1 & \Delta t^{n+1} = k_1 \Delta t^n & k_1 > 1.0 \\ if \quad m_1 \leq k \leq m_2 & \Delta t^{n+1} = \Delta t^n & \\ if \quad m_2 \leq k & \Delta t^{n+1} = k_2 \Delta t^n & k_2 < 1.0 \end{cases} \tag{19}$$

200
201   where k_1, k_2, m_1, m_2 are user-defined constants.

202   Other heuristic time step management procedures have been suggested by Kirkland et al.,

203   (1992) based on the water volumes exchanged between the adjacent cells of the grid and by

204   Ross (2003), where the time step size is controlled by the maximum allowed change in the

205   saturation.

206   For the Ross method, the fluxes are computed first and the time step magnitude is calculated

207   accordingly using

208
$$\Delta t^{n+1} = \frac{\Delta S_{max}}{\max_i \left(\dfrac{\left| q_{-,i}^n - q_{+,i}^n \right|}{\Delta z_i \left(\theta_{s,i} - \theta_{r,i} \right)} \right)} \tag{20}$$

209   where ΔS_{max} is the user-defined maximum saturation change. After the computation of the

210   actual change in the saturation, the time step is modified if the maximum of the actual change

211   exceeds $(1 + \lambda) \, max_i \left(\left| \Delta S_i \right| \right)$ where λ is a user-defined value, according to:

212
$$\Delta t^{n+1,k} = \frac{\Delta S_{max}}{\max_i \left(\left| \Delta S_i \right| \right)} \Delta t^{n+1,k-1} \tag{21}$$

213   and the system of equations is solved again. More details about handling the fluxes at

214   boundaries and saturated conditions can be found in Crevoisier et al. (2009), Ross (2003) and

215   Varado et al. (2006b).

216

217   Adaptive time stepping strategies based on time truncation error control were found to be

218   superior to others approaches (Hirthe and Graf, 2012; Kavetski et al., 2001; Tocci et al.,

219   1997). The Method of Lines using the DASPK integrator was applied to the Richards'

220   equation by Matthews et al. (2004), Miller et al. (1998), Tocci et al. (1997) among others. The

221   Method of Lines consists of discretization of the spatial part of the PDE only, leading to a

222   system of ordinary differential equations. It has been found to be significantly more efficient

223   than other temporal discretizations (Miller et al., 2006). However, Kavetski and Binning

224   (2002b) reported difficulties in obtaining convergence for the DASPK solver associated with

225   an arithmetic mean of inter-block conductivities for the most difficult problem addressed by

226   Miller et al. (1998).

227   The adaptive scheme used in this work evaluates the time steps through truncation error due

228   to the temporal discretization as proposed by Thomas and Gladwell (1988). This scheme was

229   already applied to the pressure-based formulation by Kavetski et al. (2001) and to the

230   moisture-based formulation by Kavetski and Binning (2004).

231   The difference between the first-order and second-order time approximations can be

232   considered as an estimate of the local truncation error of the first-order scheme. The first-

233   order approximation is given by:

$$\boldsymbol{\psi}_{(1)}^{n+1} = \boldsymbol{\psi}^n + \Delta t^{n+1} \frac{\partial \boldsymbol{\psi}^n}{\partial t} \qquad (22)$$

235   The second-order approximation is:

$$\begin{aligned} \boldsymbol{\psi}_{(2)}^{n+1} &= \boldsymbol{\psi}^n + \Delta t^{n+1} \frac{\partial \boldsymbol{\psi}^n}{\partial t} + \frac{1}{2}\left(\Delta t^{n+1}\right)^2 \frac{\partial^2 \boldsymbol{\psi}^n}{\partial t^2} \\ &= \boldsymbol{\psi}^n + \frac{1}{2}\left(\Delta t^{n+1}\right)\left[\frac{\partial \boldsymbol{\psi}^{n+1}}{\partial t} + \frac{\partial \boldsymbol{\psi}^n}{\partial t} \right] \end{aligned} \qquad (23)$$

237   using $\dfrac{\partial \boldsymbol{\psi}^{n+1}}{\partial t} = \dfrac{\partial \boldsymbol{\psi}^n}{\partial t} + \Delta t^{n+1} \dfrac{\partial^2 \boldsymbol{\psi}^n}{\partial t^2}$.

238   This truncation error is given by:

Hydrology and
Earth System
Sciences

Open Access

Discussions

EGU

$$\varepsilon_t^{n+1} = \max_i \left| \psi_{(2),i}^{n+1} - \psi_{(1),i}^{n+1} \right| = \frac{1}{2} \Delta t^{n+1} \max_i \left| \frac{\partial \psi_i^{n+1}}{\partial t} - \frac{\partial \psi_i^n}{\partial t} \right|$$

$$\approx \frac{1}{2} \Delta t^{n+1} \max_i \left| \frac{\psi_i^{n+1} - \psi_i^n}{\Delta t^{n+1}} - \frac{\psi_i^n - \psi_i^{n-1}}{\Delta t^n} \right|$$

239

(24)

240 When the truncation error is smaller than γ, the temporal truncation error tolerance defined by

241 the user, the size of the next time step is calculated by:

$$\Delta t^{n+1} = \Delta t^n \min \left(s \sqrt{\frac{\gamma}{\max(\varepsilon_t^{n+1}, EPS)}}, r_{max} \right)$$

242

(25)

243 When the truncation error is superior to γ, the computation is repeated with a reduced time

244 step defined as following:

$$\Delta t^n = \Delta t^n \max \left(s \sqrt{\frac{\gamma}{\max(\varepsilon_t^{n+1}, EPS)}}, r_{min} \right)$$

245

(26)

246 where r_{max} and r_{min} are user-defined constants used to avoid too drastic changes of the time

247 step. s is considered to be a safety factor that ensures that the time step changes are

248 reasonable. EPS is used to avoid floating point errors when the truncation error becomes too

249 small.

250

251 **5. Evaluation of the algorithms' performance**

252 We applied the NR method to the mixed form of RE using the standard iterative algorithm

253 and the time-adaptive algorithm. Implicit standard finite volumes have been used to solve the

254 partial differential equation and arithmetic means are used to compute the inter-block

255 hydraulic conductivity. The detailed discretizations of the matrix $\mathbf{R}'(\psi^{n+1,k})$ and the vector

256 $\mathbf{R}(\psi^{n+1,k})$ (see Eq. (18)) are given in Appendix 1. The time-adaptive algorithms have been

257 applied as described by the authors: Ross (2003) for the time stepping based on the saturation

258 changes and Kavetski et al. (2001) for the time stepping based on the truncation errors.

259 For the standard iterative algorithm, we defined two types of errors to check the convergence:

260 the error based on the maximum change of the state variables between two iterations defined

261 by $\varepsilon_\psi = \max_i \left| \psi_i^{n+1,k+1} - \psi_i^{n+1,k} \right|$ and the truncation error ε_t defined by Eq. (24). Convergence is

262 assumed to be achieved when:

$$\varepsilon_\psi < \tau_a + \tau_r \left| \psi_{imax}^{n+1,k+1} \right| \qquad (27)$$

264 where τ_a and τ_r are the absolute and relative user-defined tolerances and $\psi_{imax}^{n+1,k+1}$ is the

265 pressure corresponding to ε_ψ and when:

$$\varepsilon_t < \tau_a + \tau_r \left| \psi_{imax}^{n+1,k+1} \right| \qquad (28)$$

267 where the parameters have the same meaning as those for the previous criterion but $\psi_{imax}^{n+1,k+1}$

268 represents the pressure value corresponding to ε_t.

269 The tested algorithms are summarized in Table 1. Computations of all possible combinations

270 for the standard iterative scheme have been performed. We present only the four most

271 efficient algorithms.

272 We investigated three one-dimensional problems with various initial and boundary conditions

273 and hydraulic functions to assess the accuracy, efficiency and computational costs of the

274 different algorithms. The selected test cases represent a range of difficult infiltration problems

275 widely analyzed in the literature:

276   - TC1: infiltration in a homogeneous initially dry soil with constant prescribed pressure

277   at the surface and prescribed pressure at the bottom (Celia et al., 1990);

278   -   TC2: infiltration in a homogeneous soil initially at hydrostatic equilibrium with a

279   prescribed constant flux at the soil surface and prescribed pressure at the bottom

280   (Miller et al., 1998);

281   -   TC3: infiltration/evaporation in an initially dry heterogeneous soil, with variable

282   positive and negative fluxes at the surface and free drainage at the base of the soil

283   column (Lehmann and Ackerer, 1998).

284   For the three test cases, the soil hydraulic functions were described by Mualem-Van

285   Genuchten models (Mualem, 1976; van Genuchten, 1980), see Eq. (4) and (5).

286   The required parameters, boundary conditions and initial conditions are summarized in Table

287   2. The evolution of the relative hydraulic conductivity, the water saturation and the specific

288   moisture capacity with respect to the pressure values are shown in Figures 1, 2 and 3,

289   respectively. For TC1, the pressure will vary from -1000 cm to -75 cm only due to the

290   specific conditions of this test case. Therefore, the parameter variations are smaller than those

291   for the other test cases. Since the parameters' variations are more abrupt for test cases 2 and 3,

292   their solutions are more challenging.

293   Preliminary tests were performed to define the optimal spatial discretization. We assume that

294   the errors are only originated from the time step size and the linearization.

295   The following criteria were used for the time stepping strategy:

296   - k_1=0.80, k_2=1.20, m_1=5, m_2=10, which are the usual values for the heuristic strategy

297   defined by Eq. (19);

298   - r_{min}=0.10, r_{max}=4.0, s=0.9, EPS=10^{-10}, which are the standard values for the time

299   stepping scheme based on time discretization error defined by Eq. (26) (Kavetski et

300   al., 2001);

Hydrology and
Earth System
Sciences
Discussions

301   -   the maximum change in saturation has been evaluated using the maximum change in

302   the pressure according to the following relationship:

303
$$\Delta S_{max} \approx \frac{1}{\left(\theta_{s,imax} - \theta_{r,imax}\right)} \frac{d\theta}{d\psi}\bigg|_{imax}^{n} \left(\tau_a + \tau_r \left|\psi_{imax}^{n+1,k+1}\right|\right) \qquad (29)$$

304   The simulations have been performed using different values of τ_r and with $\tau_a = 0.0$.

305

306   We used several criteria to evaluate the performance of these codes. A typical error used in

307   solving RE is the global cumulative mass balance error defined by:

308
$$\text{MB}(t^{n+1}) = \frac{\sum_{i=1}^{M}\Delta z_i \left(\theta_i^{n+1} - \theta_i^{0}\right)}{\sum_{k=1}^{n+1}\left(q_{in}^{k} - q_{out}^{k}\right)\Delta t^{k}} \qquad (30)$$

309   where Δz_i is the size of the cell/element i, θ_i^{n+1} is its water content at time t^{n+1}, θ_i^{0} is the

310   initial water content, and q_{in}^{k} and q_{out}^{k} are the inflow and outflow, respectively, at the domain

311   boundaries at time t^k. M is the number of cells/elements. The fluxes at the boundaries are

312   defined by $q^k = \frac{1}{2}\left(q^k + q^{k-1}\right)$. The mass balance errors were checked for each runs but were

313   found to be negligible since we solved the mass-conserving RE form.

314   While it is necessary to satisfy the global mass balance for an accurate numerical scheme, a

315   low mass balance error is not sufficient to ensure the accuracy of the solution. Therefore,

316   solutions have also been compared with the reference solution obtained using a very fine

317   temporal discretization and the iterative Newton-Raphson method. This comparison is based

318   on the average relative error defined by:

Hydrology and
Earth System
Sciences

Discussions

Open Access

EGU

319
$$\varepsilon_k = \left[\frac{1}{M} \sum_i \frac{\left| \psi_i^{ref} - \hat{\psi}_i \right|^k}{\left| \psi_i^{ref} \right|^k} \right]^{1/k}$$
(31)

320 where M is the number of cells, $\boldsymbol{\psi}^{ref}$ is the reference solution and $\hat{\boldsymbol{\psi}}$ is the tested numerical

321 solution. ε_1 represents the average absolute relative error (called L_1-norm in the following),

322 ε_2 is the average quadratic error (L_2-norm) and ε_∞ is the highest local relative difference

323 between the numerical and the reference solutions (L_∞-norm).

324 Since the time-adaptive algorithm does not require the computation of the parameters and

325 their derivatives during the iterative procedure, we use N_{sol} to denote the number of times

326 where the system of equations is solved and N_{param} to denote the number of times where the

327 parameters are computed. Of course, these counters are equal to each other for the standard

328 algorithm and N_{param} is less than N_{sol} for the time-adaptive algorithm. For comparison

329 purposes, the computational costs are estimated by N_{sol} for the standard algorithm and by (N_{sol}

330 $+N_{param}$)/2 for the time-adaptive algorithm. The efficiency of the algorithms have been

331 evaluated by comparing the computational costs for a given relative tolerance τ_r. The errors

332 are presented in the tables and the figures. The figures show some additional results not listed

333 in the tables that already contains much information.

334

335 *TC1: Infiltration in a homogenous soil with constant boundary conditions*

336 This test case simulates an infiltration into a homogeneous porous medium. This problem is

337 addressed here because it has been widely analyzed previously by many authors like

338 Bouchemella et al. (2015), Celia et al. (1990), El Kadi and Ling (1993), Rathfelder and

339 Abriola, (1994), Tocci et al. (1997), among others. The computations were performed with a

340   spatial discretization of 0.1 cm. The initial time step size was set to 1.0 10^{-5} s, and the

341   maximum time step size was set to 400 s.

342   The results for the iterative and time-adaptive algorithms are presented in Tables 3 and 4,

343   respectively. When both convergence criteria are used (algorithms SH_Δψ_Δt and

344   SS_Δψ_Δt), N_{trunc} represents the number of times where the truncation error is the most

345   restrictive condition. For the heuristic time stepping schemes, the convergence is mostly

346   linked to the truncation error (N_{trunc} is close to N_{sol}), whereas when the saturation time

347   stepping scheme is used, the most restrictive criterion is the maximum difference in the

348   pressure.

349   When the time stepping scheme is based on saturation, for both iterative and time-adaptive

350   algorithms, the number of iterations required to solve the problem is proportional to the

351   relative tolerance. Therefore, highly accurate solutions incur high computational costs.

352   For the time-adaptive scheme, the number of parameter changes N_{param} is close to the number

353   of iterations for low tolerance values. Small tolerance values lead to small time steps,

354   avoiding time step adjustments. This is not the case for larger tolerance values that lead to

355   larger time steps and therefore to additional iterations (see for example TA_T for the

356   tolerance of $\tau_r = 10^{-2}$ – Table 4).

357   The three types of errors provide the same information. The best solution for one type of error

358   is also the best solution for the two others.

359   On average, the iterative algorithm is faster than the time-adaptive algorithm that requires

360   more iterations for a given error. This is also shown in Figure 4 that presents the convergence

361   rate of the L_2-norm with respect to the computational costs, *i.e.,* the number of iterations or

362   number of iterations and number of parameter changes. The time-adaptive algorithm with

363   time stepping based on the truncation errors performs quite poorly compared to the other

Hydrology and
Earth System
Sciences
Discussions

Open Access

EGU

364 algorithms. Irrespective of the tolerance, this algorithm leads to a wetting front moving faster

365 (Fig. 5).

366 When the relative tolerance is set to a very low value ($\tau_r = 10^{-5}$), the iterative scheme with

367 time stepping based on the saturation changes shows behavior that is different from that found

368 for the less restrictive tolerance. The criterion based on truncation errors is no longer

369 significant ($N_{trunc}=252$), possibly explaining why the accuracy of the scheme remains

370 constant. This also indicates that errors due to time discretization have to be handled, either in

371 the convergence criterion or in the time stepping strategy.

372 For this test case, the most efficient algorithms are the iterative algorithms using the time

373 stepping strategy based on truncation error (ST_Δψ) or based on the saturation changes

374 (SS_Δψ_Δt), except for the case of very high precision where ST_Δψ outperforms the other

375 algorithms.

376

377 *TC2: Infiltration in a homogenous soil with hydrostatic initial conditions*

378 This test case models an infiltration in a 200 cm vertical column of unconsolidated clay loam

379 with non-uniform grain size distribution and was considered by Miller et al. (1998) to be a

380 very challenging test. This problem was found to be more challenging from the numerical

381 point of view compared to TC1 due to the relative permeability function that enhances the

382 non-linear behavior of Richards' equation (Fig. 1, 2, 3). The cell size has been set to 0.125

383 cm, the initial time step to 10^{-5}s and the maximum time step magnitude to 1000 s.

384 The different norms for the iterative and the time-adaptive schemes are given in Tables 5 and

385 6.

386 Investigation of this test case leads to similar qualitative conclusions when the time stepping

387 scheme is based on the saturation differences (SS_Δψ_Δt and TA_S). The standard scheme

Hydrology and
Earth System
Sciences
Open Access
Discussions
EGU

388   SH_$\Delta\psi$ fails to provide an accurate solution within a reasonable number of iterations (less

389   than 10^7).

390   The most efficient methods are the schemes using the time stepping strategy based on

391   truncation errors (Fig. 6). However, as found for TC1, the adaptive time algorithm failed to

392   provide highly accurate results (L_2-norm error less than approximately 4.5 10^{-4}).

393   Figure 7 shows the time step magnitudes for approximately equal L_2-norms for the two time-

394   adaptive algorithms and for the iterative algorithm using truncation errors for time stepping

395   (4.254 10^{-4} within 3503 iterations for ST_$\Delta\psi$, 4.563 10^{-4} within 3094 iterations for TA_T and

396   4.844 10^{-4} within 113583 iterations for TA_S). The increase in the time step length after 10 s

397   is the same, irrespective of the algorithm. For a smaller time, both truncation time stepping

398   strategies differ for the estimate of the first time step only. The scheme using the saturation

399   based time stepping is penalized by the poor estimate of the first maximum allowed saturation

400   change. This leads to the estimate of the first time step magnitude that was too long for

401   reaching convergence.

402

403   *TC3: Infiltration/evaporation in a heterogeneous soil*

404   This case study simulates infiltration in an initially dry heterogeneous soil with a succession

405   of rainfall and evaporations as upper boundary conditions during 35 days. This problem

406   differs from the two previous cases by the soil heterogeneity and also by the non-monotonic

407   boundary conditions at the soil surface. It is expected that non-monotonic discontinuous

408   boundary conditions will increase the difficulty of finding accurate solutions. The soil profile

409   consists of three 60 cm thick layers. The layers are discretized using cells with the size of 0.10

410   cm. The maximum time step magnitude is chosen as 0.20 days to avoid a too rough

411   discretization of the upper boundary conditions. The initial time step is set to 10^{-5} day.

412   The relative errors estimated by the iterative algorithms and the time-adaptive algorithms are

413   presented in Tables 7 and 8, respectively, and are plotted in Figure 8.

414   The standard iterative scheme fails to converge within the maximum number of iterations

415   (10^7) when the tolerance is not sufficiently restrictive. The detailed analyses of the

416   computation showed that the time step size was quite large compared to the more restrictive

417   conditions until day 28.0 where the infiltration fluxes were equal to 1.50 cm/day and where

418   the conditions were near saturation due to the previous infiltration period. This led to a

419   decrease of the time step to close to the minimum value (10^{-8} s), causing the procedure to

420   stop. More restrictive conditions lead to smaller time steps from the beginning of the

421   simulation and a better approximation of the solutions during the entire simulation.

422   The iterative scheme coupled with the truncation based time step strategy showed a

423   surprisingly unstable behavior for $\tau_r = 10^{-3}$. The scheme did not converge for

424    $\tau_r \in \left[0.96\,10^{-3} ; 1.04\,10^{-3} \right]$. The results presented in Table 7 and Figure 8 are obtained for

425    $\tau_r = 0.90\,10^{-3}$. At this stage of our work, we were not able to provide a meaningful

426   explanation for this effect.

427   The time-adaptive algorithm with the saturation based time stepping scheme is the most

428   efficient for an L_2-norm greater than 10^{-4}. For more accurate results, the iterative method with

429   the time stepping strategy using the truncation error must be preferred. The impact of the time

430   stepping strategy for these two algorithms is shown in Figure 9 for approximately the same

431   L_2-norm (2.051 10^{-3} within 1283 iterations for TA_S and 1.517 10^{-3} within 6504 iterations for

432   ST_$\Delta\psi$). The time step changes is related to the boundary conditions variations as expected.

433   The strategy based on the saturation variation leads to a longer time step than the strategy

434   using the time truncation error. This difference can be quite important (see the simulation

435   between days 25 and 30). The consequences of this difference are a reduced number of

436   iterations but also a less accurate computation, irrespective of the error norm.

437

438   **6. Summary and conclusions**

439   The solution of RE is complex and very time consuming due to its highly non-linear

440   properties. Several algorithms have been tested for the mixed-form of Richards equation,

441   including time-adaptive methods. Based on the numerical examples that differ in their

442   parameters (level of non-linearity) and in their initial and boundary conditions, the

443   conclusions and recommendations are:

444   1. Our numerical developments showed that the method suggested by Ross (2003) in its

445   implicit formulation can be considered as a Newton-Raphson method with a time-

446   adaptive algorithm.

447   2. The different algorithms have different convergence rates (accuracy improvement of

448   the scheme as a function of the computational costs). Therefore, an algorithm can be

449   very efficient for a given accuracy and less efficient for another level of precision.

450   3. The mass balance is not a good criterion for the evaluation of the results because the

451   mixed-form preserves the mass balance, irrespective of the pressure distribution

452   within the profile.

453   4. The use of both criteria (ε_ψ, the maximum variable difference between two iterations,

454   ε_t the time truncation error) should be implemented in the iterative procedure. The use

455   of ε_ψ only, which is the case in many numerical codes, does not provide any

456   information about the accuracy of the time derivative approximation.

457   5. Our 1-dimensional examples did not show a significant advantage of the time-adaptive

458   algorithm that avoids the computation of the parameters for each iteration. However,

459   this may depend on the number of elements used for the spatial discretization, and this

460   conclusion may be different for 2D or 3D domains.

461

462   Depending on the type of the problem that must be solved (parameters behavior with respect

463   to the pressure, time variations of the boundary conditions), the time truncation errors may be

464   predominant compared to the error corresponding to the pressure changes between two

465   iterations. Therefore, we recommend the use of both types of errors by implementing the

466   truncation errors either in the convergence procedure (convergence reached if ε_ψ and ε_t are

467   smaller than a user's defined tolerance) or in the time stepping strategy as defined by

468   Kavetski et al. (2001).

469

470

References

Bause, M., Knabner, P., 2004. Computation of variably saturated subsurface flow by adaptive mixed hybrid finite element methods. Adv. Water Resour. 27, 565–581. doi:10.1016/j.advwatres.2004.03.005

Belfort, B., Younes, A., Fahs, M., Lehmann, F., 2013. On equivalent hydraulic conductivity for oscillation–free solutions of Richard's equation. J. Hydrol. 505, 202–217. doi:10.1016/j.jhydrol.2013.09.047

Bergamaschi, L., Putti, M., 1999. Mixed finite elements and Newton-type linearizations for the solution of Richards' equation. Int. J. Numer. Methods Eng. 45, 1025–1046. doi:10.1002/(SICI)1097-0207(19990720)45

Bouchemella, S., Seridi, A., Alimi-Ichola, I., 2015. Numerical simulation of water flow in unsaturated soils: comparative study of different forms of Richards's equation. Eur. J. Environ. Civ. Eng. 19, 1–26. doi:10.1080/19648189.2014.926294

Celia, M.A., Bouloutas, E.T., Zarba, R.L., 1990. A general mass-conservative numerical solution for the unsaturated flow equation. Water Resour. Res. 26, 1483–1496. doi:10.1029/WR026i007p01483

Crevoisier, D., Chanzy, A., Voltz, M., 2009. Evaluation of the Ross fast solution of Richards' equation in unfavourable conditions for standard finite element methods. Adv. Water Resour. 32, 936–947. doi:10.1016/j.advwatres.2009.03.008

Diersch, H.-J.G., Perrochet, P., 1999. On the primary variable switching technique for simulating unsaturated–saturated flows. Adv. Water Resour. 23, 271–301. doi:10.1016/S0309-1708(98)00057-8

El Kadi, A.I., Ling, G., 1993. The Courant and Peclet Number criteria for the numerical solution of the Richards Equation. Water Resour. Res. 29. doi:10.1029/93WR00929

Fahs, M., Younes, A., Lehmann, F., 2009. An easy and efficient combination of the Mixed Finite Element Method and the Method of Lines for the resolution of Richards' Equation. Environ. Model. Softw. 24, 1122–1126. doi:10.1016/j.envsoft.2009.02.010

Farthing, M.W., Kees, C.E., Miller, C.T., 2003. Mixed finite element methods and higher order temporal approximations for variably saturated groundwater flow. Adv. Water Resour. 26, 373–394. doi:10.1016/S0309-1708(02)00187-2

Feddes, R.A., Kabat, P., Van Bakel, P.J.T., Bronswijk, J.J.B., Halbertsma, J., 1988. Modelling soil water dynamics in the unsaturated zone — State of the art. J. Hydrol. 100, 69–111. doi:10.1016/0022-1694(88)90182-5

Forsyth, P.A., Wu, Y.S., Pruess, K., 1995. Robust numerical methods for saturated-unsaturated flow with dry initial conditions in heterogeneous media. Adv. Water Resour. 18, 25–38. doi:10.1016/0309-1708(95)00020-J

Gottardi, G., Venutelli, M., 2001. UPF: two-dimensional finite-element groundwater flow model for saturated–unsaturated soils. Comput. Geosci. 27, 179–189. doi:10.1016/S0098-3004(00)00082-0

Hirthe, E.M., Graf, T., 2012. Non-iterative adaptive time-stepping scheme with temporal truncation error control for simulating variable-density flow. Adv. Water Resour. 49, 46–55. doi:10.1016/j.advwatres.2012.07.021

Kavetski, D., Binning, P., 2004. Truncation error and stability analysis of iterative and non-iterative Thomas–Gladwell methods for first-order non-linear differential equations. Int. J. Numer. Methods Eng. 60, 2031–2043. doi:10.1002/nme.1035

Kavetski, D., Binning, P., 2002a. Adaptive backward Euler time stepping with truncation error control for numerical modelling of unsaturated fluid flow. Int. J. Numer. Methods Eng. 53, 1301–1322. doi:10.1002/nme.329

Kavetski, D., Binning, P., 2002b. Noniterative time stepping schemes with adaptive truncation error control for the solution of Richards equation. Water Resour. Res. 38. doi:10.1029/2001WR000720

Kavetski, D., Binning, P., Sloan, S.W., 2001. Adaptive time stepping and error control in a mass conservative numerical solution of the mixed form of Richards equation. Adv. Water Resour. 24, 595–605. doi:10.1016/S0309-1708(00)00076-2

Kirkland, M.R., Hills, R.G., Wierenga, P.J., 1992. Algorithms for solving Richards' equation for variably saturated soils. Water Resour. Res. 28, 2049–2058.

Lehmann, F., Ackerer, P., 1998. Comparison of Iterative Methods for Improved Solutions of the Fluid Flow Equation in Partially Saturated Porous Media. Transp. Porous Media 31, 275–292. doi:10.1023/A:1006555107450

Matthews, C.J., Braddock, R.D., Sander, G.C., 2004. Modeling flow through a one-dimensional multi-layered soil profile using the Method of Lines. Environ. Model. Assess. 9, 103–113.

Miller, C.T., Abhishek, C., Farthing, M.W., 2006. A spatially and temporally adaptive solution of Richards' equation. Adv. Water Resour. 29, 525–545. doi:10.1016/j.advwatres.2005.06.008

Miller, C.T., Williams, G.A., Kelley, C.T., Tocci, M.D., 1998. Robust solution of Richards' equation for nonuniform porous media. Water Resour. Res. 34, 2599–2610. doi:10.1029/98WR01673

Mualem, Y., 1976. A new model for predicting the hydraulic conductivity of unsaturated porous media. Water Resour. Res. 12, 513–522. doi:10.1029/WR012i003p00513

Paniconi, C., Aldama, A.A., Wood, E.F., 1991. Numerical evaluation of iterative and noniterative methods for the solution of the nonlinear Richards equation. Water Resour. Res. 27, 1147–1163.

Paniconi, C., Putti, M., 1994. A comparison of Picard and Newton iteration in the numerical solution of multidimensional variably saturated flow problems. Water Resour. Res. 30, 3357–3374. doi:10.1029/94WR02046

R. G. Hills, I.P., 1989. Modeling one-dimensional infiltration into very dry soils: 1. Model development and evaluation. Water Resour. Res. 25. doi:10.1029/WR025i006p01259

Rathfelder, K., Abriola, L.M., 1994. Mass conservative numerical solutions of the head-based Richards equation. Water Resour. Res. 30, 2579–2586. doi:10.1029/94WR01302

Richards, L.A., 1931. Capillary conduction of liquids through porous medium. J. Appl. Phys. 1, 318–333. doi:10.1063/1.1745010

Romano, N., Brunone, B., Santini, A., 1998. Numerical analysis of one-dimensional unsaturated flow in layered soils. Adv. Water Resour. 21, 315–324. doi:10.1016/S0309-1708(96)00059-0

Ross, P.J., 2003. Modeling Soil Water and Solute Transport—Fast, Simplified Numerical Solutions. Agron. J. 95, 1352. doi:10.2134/agronj2003.1352

Ross, P.J., Bristow, K.L., 1990. Simulating Water Movement in Layered and Gradational Soils Using the Kirchhoff Transform. Soil Sci. Soc. Am. J. 54, 1519. doi:10.2136/sssaj1990.03615995005400060002x

Thomas, R.M., Gladwell, I., 1988. Variable-order variable-step algorithms for second-order systems. Part 1: The methods. Int. J. Numer. Methods Eng. 26, 39–53.

Tocci, M.D., Kelley, C.T., Miller, C.T., 1997. Accurate and economical solution of the pressure-head form of Richards' equation by the method of lines. Adv. Water Resour. 20, 1–14. doi:10.1016/S0309-1708(96)00008-5

van Dam, J.C., Feddes, R.A., 2000. Numerical simulation of infiltration, evaporation and shallow groundwater levels with the Richards equation. J. Hydrol. 233, 72–85. doi:10.1016/S0022-1694(00)00227-4

van Genuchten, M.T., 1980. A Closed-form Equation for Predicting the Hydraulic Conductivity of Unsaturated Soils1. Soil Sci. Soc. Am. J. 44, 892. doi:10.2136/sssaj1980.03615995004400050002x

Varado, N., Braud, I., Ross, P.J., 2006a. Development and assessment of an efficient vadose zone module solving the 1D Richards' equation and including root extraction by plants. J. Hydrol. 323, 258–275. doi:10.1016/j.jhydrol.2005.09.015

Varado, N., Braud, I., Ross, P.J., Haverkamp, R., 2006b. Assessment of an efficient numerical solution of the 1D Richards' equation on bare soil. J. Hydrol. 323, 244–257. doi:10.1016/j.jhydrol.2005.07.052

Williams, G.A., Miller, C.T., Kelley, C.T., 2000. Transformation approaches for simulating flow in variably saturated porous media. Water Resour. Res. 36, 923–934. doi:10.1029/1999WR900349

Zha, Y., Shi, L., Ye, M., Yang, J., 2013. A generalized Ross method for two- and three-dimensional variably saturated flow. Adv. Water Resour. 54, 67–77. doi:10.1016/j.advwatres.2013.01.002

Zha, Y., Tso, M.C.-H., Shi, L., Yang, J., 2015. Comparison of Non iterative Algorithms Based on Different Forms of Richards' Equation. Environ. Model. Assess. 21, 357–370. doi:10.1007/s10666-015-9467-1

1   **APPENDIX 1.**
2

3   The numerical method used in the paper is implicit standard finite difference. For a cell i of

4   the grid, the unsaturated flow equation (4) can be discretized in the following way:

5

6
$$
\begin{cases}
\dfrac{\theta_i^{n+1} - \theta_i^n}{\Delta t} + S_w s_0 \dfrac{\psi_i^{n+1} - \psi_i^n}{\Delta t} + \dfrac{q_{i+}^{n+1} - q_{i-}^{n+1}}{\Delta z_i} = f_i \\[3mm]
q_{i-}^{n+1} = -K_{i-}\left(\dfrac{\psi_i^{n+1} - \psi_{i-1}^{n+1}}{\Delta z_{i-}} - 1 \right) \\[3mm]
q_{i+}^{n+1} = -K_{i+}\left(\dfrac{\psi_{i+1}^{n+1} - \psi_i^{n+1}}{\Delta z_{i+}} - 1 \right)
\end{cases}
\tag{A32}
$$

7

8   where n is the time step, K_{i-} is the inter-block conductivity between cell i and (i-1) defined by

9       $K_{i-} = \dfrac{\Delta z_{i-1} K(\psi_{i-1}) + \Delta z_i K(\psi_i)}{\Delta z_{i-1} + \Delta z_i}$, K_{i+} is the inter-block conductivity between cell i and (i+1)

10   defined by $K_{i+} = \dfrac{\Delta z_i K(\psi_i) + \Delta z_{i+1} K(\psi_{i+1})}{\Delta z_i + \Delta z_{i+1}}$. $\Delta z_{i-} = \dfrac{1}{2}\left(\Delta z_{i-1} + \Delta z_i\right)$ is the distance between the

11   center of cell (i-1) and i. $\Delta z_{i+} = \dfrac{1}{2}\left(\Delta z_i + \Delta z_{i+1}\right)$ is the distance between the center of cell i and

12   (i+1).
13
14
15   The residual is:
16
17      $R(\psi_i^{n+1,k}) = \Delta z_i \left(\theta_i^{n+1,k} - \theta_i^n \right) + \Delta z_i S_w s_0 \left(\psi_i^{n+1,k} - \psi_i^n \right) + \Delta t \left(q_{i+}^{n+1,k} - q_{i-}^{n+1,k} \right) - \Delta t \Delta z_i f_i$ (A33)
18
19   where k is the iteration counter.
20
21   The residual derivatives are:
22

23
$$
\begin{aligned}
\frac{\partial R(\psi_i^{n+1,k})}{\partial \psi_{i-1}^{n+1,k}} &= -\Delta t \frac{\partial q_{i-}^{n+1,k}}{\partial \psi_{i-1}^{n+1,k}} \\[2mm]
\frac{\partial R(\psi_i^{n+1,k})}{\partial \psi_i^{n+1,k}} &= \Delta z_i \frac{d\theta_i^{n+1,k}}{d\psi_i^{n+1,k}} + \Delta z_i S_w s_0 + \Delta t \left(\frac{\partial q_{i+}^{n+1,k}}{\partial \psi_i^{n+1,k}} - \frac{\partial q_{i-}^{n+1,k}}{\partial \psi_i^{n+1,k}} \right) \\[2mm]
\frac{\partial R(\psi_i^{n+1,k})}{\partial \psi_{i+1}^{n+1,k}} &= \Delta t \frac{\partial q_{i+}^{n+1,k}}{\partial \psi_{i+1}^{n+1,k}}
\end{aligned}
\tag{A34}
$$

24
25   Therefore, the system to solve is:
26

Hydrology and
Earth System
Sciences

Open Access

Discussions

EGU

27

$$-\Delta t \frac{\partial q_{i-}^{n+1,k}}{\partial \psi_{i-1}^{n+1,k}} \Delta \psi_{i-1}^{n+1,k+1} +$$

$$\left[\Delta z_i \frac{d\theta_i^{n+1,k}}{d\psi_i^{n+1,k}} + \Delta z_i S_w s_0 + \Delta t \left(\frac{\partial q_{i+}^{n+1,k}}{\partial \psi_i^{n+1,k}} - \frac{\partial q_{i-}^{n+1,k}}{\partial \psi_i^{n+1,k}} \right) \right] \Delta \psi_i^{n+1,k+1} +$$

$$\Delta t \frac{\partial q_{i+}^{n+1}}{\partial \psi_{i+1}^{n+1,k}} \Delta \psi_{i+1}^{n+1,k+1} =$$

$$-\Delta z_i \left(\theta_i^{n+1,k} - \theta_i^n \right) - \Delta z_i S_w s_0 \left(\psi_i^{n+1,k} - \psi_i^n \right) - \Delta t \left(q_{i+}^{n+1,k} - q_{i-}^{n+1,k} \right) + \Delta t \Delta z_i f_i$$

28
(A35)
29
30   With the following derivatives of the fluxes $q_{i-}^{n+1,k}$
31
32

$$\begin{cases} \dfrac{\partial q_{i-}^{n+1,k}}{\partial \psi_{i-1}^{n+1,k}} = -\dfrac{\partial K_{i-}^{n+1,k}}{\partial \psi_{i-1}^{n+1,k}} \left(\dfrac{\psi_i^{n+1,k} - \psi_{i-1}^{n+1,k}}{\Delta z_{i-}} - 1 \right) + \dfrac{K_{i-}^{n+1,k}}{\Delta z_{i-}} \\[3mm] \dfrac{\partial q_{i-}^{n+1,k}}{\partial \psi_i^{n+1,k}} = -\dfrac{\partial K_{i-}^{n+1,k}}{\partial \psi_i^{n+1,k}} \left(\dfrac{\psi_i^{n+1,k} - \psi_{i-1}^{n+1,k}}{\Delta z_{i-}} - 1 \right) - \dfrac{K_{i-}^{n+1,k}}{\Delta z_{i-}} \end{cases}$$

(A36)

33
34   and $q_{i+}^{n+1,k}$:
35
36

$$\begin{cases} \dfrac{\partial q_{i+}^{n+1,k}}{\partial \psi_i^{n+1,k}} = -\dfrac{\partial K_{i+}^{n+1,k}}{\partial \psi_i^{n+1,k}} \left(\dfrac{\psi_{i+1}^{n+1,k} - \psi_i^{n+1,k}}{\Delta z_{i+}} - 1 \right) + \dfrac{K_{i+}^{n+1,k}}{\Delta z_{i+}} \\[3mm] \dfrac{\partial q_{i+}^{n+1,k}}{\partial \psi_{i+1}^{n+1,k}} = -\dfrac{\partial K_{i+}^{n+1,k}}{\partial \psi_{i+1}^{n+1,k}} \left(\dfrac{\psi_{i+1}^{n+1,k} - \psi_i^{n+1,k}}{\Delta z_{i+}} - 1 \right) - \dfrac{K_{i+}^{n+1,k}}{\Delta z_{i+}} \end{cases}$$

(A37)

37
38   The component of the vector of the residuals $\mathbf{R}$ is given by equation (A33) and the
39   coefficients of the matrix $\mathbf{R}'$ for cell i are:
40

$$R'_{i-1,i} = \Delta t \left[\frac{\partial K_{i-}^{n+1,k}}{\partial \psi_{i-1}^{n+1,k}} \left(\frac{\psi_i^{n+1,k} - \psi_{i-1}^{n+1,k}}{\Delta z_{i-}} - 1 \right) - \frac{K_{i-}^{n+1,k}}{\Delta z_{i-}} \right]$$

$$R'_{i,i} = \Delta z_i \left[\frac{d\theta_i^{n+1,k}}{d\psi_i^{n+1,k}} + S_w s_0 \right] - \Delta t \left[\frac{\partial K_{i+}^{n+1,k}}{\partial \psi_i^{n+1,k}} \left(\frac{\psi_{i+1}^{n+1,k} - \psi_i^{n+1,k}}{\Delta z_{i+}} - \right) - \frac{K_{i+}^{n+1,k}}{\Delta z_{i+}} \right]$$

41
(A38)

$$+\Delta t \left[\frac{\partial K_{i-}^{n+1,k}}{\partial \psi_i^{n+1,k}} \left(\frac{\psi_i^{n+1,k} - \psi_{i-1}^{n+1,k}}{\Delta z_{i-}} - 1 \right) + \frac{K_{i-}^{n+1,k}}{\Delta z_{i-}} \right]$$

$$R'_{i,i+1} = -\Delta t \left[\frac{\partial K_{i+}^{n+1,k}}{\partial \psi_{i+1}^{n+1,k}} \left(\frac{\psi_{i+1}^{n+1,k} - \psi_i^{n+1,k}}{\Delta z_{i+}} - 1 \right) + \frac{K_{i+}^{n+1,k}}{\Delta z_{i+}} \right]$$

42
43   In case of prescribed flux at the upper boundary, the residual is written as:
44

45 $$R_1(\psi_1^{n+1,k}) = \Delta z_1\left[\left(\theta_1^{n+1,k} - \theta_1^n\right) + S_w s_0\left(\psi_1^{n+1,k} - \psi_1^n\right)\right] + \Delta t\left(q_{1+}^{n+1} - q_{BC}\right) - \Delta t \Delta z_1 f_1 \qquad \text{(A39)}$$

46

47 Using the derivatives as defined in (A36) and (A37), the matrix coefficients are changed as

48 follow:

49

50 $$R'_{1,1} = \Delta z_1\left(\frac{d\theta_1^{n+1,k}}{d\psi_1^{n+1,k}} + S_w s_0\right) - \Delta t\left[\frac{\partial K_{1+}^{n+1,k}}{\partial \psi_1^{n+1,k}}\left(\frac{\psi_2^{n+1,k} - \psi_1^{n+1,k}}{\Delta z_{1+}} - 1\right) - \frac{K_{1+}^{n+1,k}}{\Delta z_{1+}}\right]$$
$$R'_{1,2} = -\Delta t\left[\frac{\partial K_{1+}^{n+1,k}}{\partial \psi_2^{n+1,k}}\left(\frac{\psi_2^{n+1,k} - \psi_1^{n+1,k}}{\Delta z_{1+}} - 1\right) + \frac{K_{1+}^{n+1,k}}{\Delta z_{1+}}\right] \qquad \text{(A40)}$$

51

52 If the flux is applied at the bottom of the profile, similar developments lead to the residual:

53

54 $$R_N = \Delta z_N\left[\left(\theta_N^{n+1,k} - \theta_N^n\right) + S_w s_0\left(\psi_N^{n+1,k} - \psi_N^n\right)\right] + \Delta t\left(q_{BC} - q_{N-}^{n+1,k}\right) - \Delta t \Delta z_N f_N \qquad \text{(A41)}$$

55

56 and its derivatives

57

58 $$R'_{N-1,N} = \Delta t\left[\frac{\partial K_{N-}^{n+1,k}}{\partial \psi_{N-1}^{n+1,k}}\left(\frac{\psi_N^{n+1,k} - \psi_{N-1}^{n+1,k}}{\Delta z_{N-}} - 1\right) - \frac{K_{N-}^{n+1,k}}{\Delta z_{N-}}\right]$$
$$R'_{N,N} = \Delta z_N\left(\frac{d\theta_N^{n+1,k}}{d\psi_N^{n+1,k}} + S_w s_0\right) + \Delta t\left[\frac{\partial K_{N-}^{n+1,k}}{\partial \psi_N^{n+1,k}}\left(\frac{\psi_N^{n+1,k} - \psi_{N-1}^{n+1,k}}{\Delta z_{N-}} - 1\right) + \frac{K_{N-}^{n+1,k}}{\Delta z_{N-}}\right] \qquad \text{(A42)}$$

59

60 If the pressure is described at the top of the soil, the corresponding flux is defined by:

61

62 $$q_{1-}^{n+1,k} = -K_{1-}\left(\frac{\psi_1^{n+1,k} - \psi_{BC}}{\Delta z_1/2} - 1\right) \qquad \text{(A43)}$$

63

64 And the derivative is:

65

66 $$\frac{\partial q_{1-}^{n+1,k}}{\partial \psi_1^{n+1,k}} = -\frac{\partial K_{1-}^{n+1,k}}{\partial \psi_1^{n+1,k}}\left(\frac{\psi_1^{n+1,k} - \psi_{BC}}{\Delta z_1/2} - 1\right) - \frac{K_{1-}^{n+1,k}}{\Delta z_1/2} \qquad \text{(A44)}$$

67

68 The corresponding residual and the matrix coefficients are:

Hydrology and
Earth System
Sciences
Discussions

Open Access

EGU

69 $\quad R_1 = \Delta z_1 \left[\left(\theta_1^{n+1,k} - \theta_1^n \right) + S_w s_0 \left(\psi_1^{n+1,k} - \psi_1^n \right) \right] + \Delta t \left(q_{1+}^{n+1,k} - q_{1-}^{n+1,k} \right) - \Delta t \Delta z_1 f_1$ $\qquad$ (A45)

70 $\quad$ and

$$R'_{1,1} = \Delta z_1 \left(\frac{d\theta_1^{n+1,k}}{d\psi_1^{n+1,k}} + S_w s_0 \right) - \Delta t \left[\frac{\partial K_{1+}^{n+1,k}}{\partial \psi_1^{n+1,k}} \left(\frac{\psi_2^{n+1,k} - \psi_1^{n+1,k}}{\Delta z_{1+}} - 1 \right) - \frac{K_{1+}^{n+1,k}}{\Delta z_{1+}} \right]$$

71 $$\qquad\qquad + \Delta t \left[\frac{\partial K_{1-}^{n+1,k}}{\partial \psi_1^{n+1,k}} \left(\frac{\psi_1^{n+1,k} - \psi_{BC}}{\Delta z_1 / 2} - 1 \right) + \frac{K_{1-}^{n+1,k}}{\Delta z_1 / 2} \right]$$ $\qquad$ (A46)

$$R'_{1,2} = -\Delta t \left[\frac{\partial K_{1+}^{n+1,k}}{\partial \psi_2^{n+1,k}} \left(\frac{\psi_2^{n+1,k} - \psi_1^{n+1,k}}{\Delta z_{1+}} - 1 \right) + \frac{K_{1+}^{n+1,k}}{\Delta z_{1+}} \right]$$

72

73 $\quad$ Similarly, if the pressure is prescribed at the soils column's bottom, we have:

74

75 $\quad R_N = \Delta z_N \left[\left(\theta_N^{n+1,k} - \theta_N^n \right) + S_w s_0 \left(\psi_N^{n+1,k} - \psi_N^n \right) \right] + \Delta t \left(q_{N+}^{n+1,k} - q_{N-}^{n+1,k} \right) - \Delta t \Delta z_N f_N$ $\qquad$ (A47)

76 $\quad$ and

$$R'_{N-1,N} = \Delta t \left[\frac{\partial K_{N-}^{n+1,k}}{\partial \psi_{N-1}^{n+1,k}} \left(\frac{\psi_N^{n+1,k} - \psi_{N-1}^{n+1,k}}{\Delta z_{N-}} - 1 \right) - \frac{K_{N-}^{n+1,k}}{\Delta z_{N-}} \right]$$

77 $\quad R'_{N,N} = \Delta z_N \left(\frac{d\theta_N^{n+1,k}}{d\psi_N^{n+1,k}} + S_w s_0 \right) - \Delta t \left[\frac{\partial K_{N+}^{n+1,k}}{\partial \psi_N^{n+1,k}} \left(\frac{\psi_{BC} - \psi_N^{n+1,k}}{\Delta z_N / 2} - 1 \right) - \Delta t \frac{K_{N+}^{n+1,k}}{\Delta z_N / 2} \right]$ $\qquad$ (A48)

$$\qquad\qquad + \Delta t \left[\frac{\partial K_{N-}^{n+1,k}}{\partial \psi_N^{n+1,k}} \left(\frac{\psi_N^{n+1,k} - \psi_{N-1}^{n+1,k}}{\Delta z_{N-}} - 1 \right) + \frac{K_{N-}^{n+1,k}}{\Delta z_{N-}} \right]$$

78

79 $\quad$ The numerical code is written in FORTRAN 90 and is available upon request.

Hydrology and
Earth System
Sciences

Open Access

Discussions

List of Tables

Table 1. Different options of the tested algorithms. Reference to the corresponding equation in parenthesis.

Table 2: Domain size (L), initial conditions (IC), boundary conditions at the soil surface (BC_u) and at the soil bottom (BC_l), saturated hydraulic conductivity (K_s), residual and saturated water contents (θ_r, θ_s) and shape parameters (α, n) for the different test cases. Length and time units are centimeters and seconds.

Table 3: Relative errors and number of iterations obtained for the iterative algorithm depending on different convergence criteria for TC1.

Table 4: Relative errors and number of iterations obtained for the time-adaptive algorithm depending on different convergence criteria for TC1.

Table 5: Relative errors and number of iterations obtained for the iterative algorithm depending on different convergence criteria for TC2 (n.c.: non convergence in less than 10^7 iterations).

Table 6: Relative errors and number of iterations obtained for the time-adaptive algorithm depending on different convergence criteria for TC2.

Table 7: Relative errors and number of iterations obtained for the iterative algorithm depending on different convergence criteria for TC3 (n.c.: non convergence in less than 10^7 iterations, * convergence failed for 10^{-3}, $\tau_r = 0.90 \cdot 10^{-3}$).

Table 8: Relative errors and number of iterations obtained for the time-adaptive algorithm depending on different convergence criteria for TC3.

| | Standard iterative algorithm | | | | | Time-adaptive algorithm | |
| | Time stepping | | | Stopping criterion | | | |
	Heuristic (19)	Truncation (25) (26)	Saturation (20) (21)	Pressure (27)	Truncation (28)	Truncation (25) (26)	Saturation (20) (21)
SH_Δψ	x			x			
SH_Δψ_Δt	x			x	x		
ST_Δψ		x		x			
SS_Δψ_Δt			x	x	x		
TA_T						x	
TA_S							x

Table 1: Different options of the tested algorithms. Reference to the corresponding equation in parenthesis.

	L	IC	BC_u	BC_l	K_s	θ_r	θ_s	α	η
TC1	30	-1000.0	$\psi = -75$	$\psi = -1000$	$9.22\ 10^{-3}$	0.102	0.368	0.0335	2.0
TC2	200	z-200	$q=3.7\ 10^{-5}$	$\psi = 0$	$7.18\ 10^{-5}$	0.095	0.410	0.019	1.31
TC3	60	-100.0	q(t)	$q(t)=K_M(t)$	$6.26\ 10^{-3}$	0.0286	0.366	0.028	2.239
	60	-100.0			$1.51\ 10^{-4}$	0.106	0.469	0.0104	1.395
	60	-100.0			$6.26\ 10^{-3}$	0.0286	0.366	0.028	2.239

Table 2: Domain size (L), initial conditions (IC), boundary conditions at the soil surface (BC_u) and at the soil bottom (BC_l), saturated hydraulic conductivity (K_s), residual and saturated water contents (θ_r , θ_s) and shape parameters (α , η) for the different test cases.
$K_M(t)$ is the hydraulic conductivity of the last grid cell.
Length and time units are centimeters and seconds respectively.

Tol.	Algorithm	L_1	L_2	L_∞	N_{trunc}	N_{sol}
	SH_$\Delta\psi$	$1.918\ 10^{-3}$	$8.829\ 10^{-3}$	0.106		2177
10^{-5}	SH_$\Delta\psi$_Δt	$8.391\ 10^{-6}$	$6.459\ 10^{-5}$	$8.782\ 10^{-4}$	542371	615880
	ST_$\Delta\psi$	$3.968\ 10^{-4}$	$1.045\ 10^{-3}$	$3.512\ 10^{-3}$		6160
	SS_$\Delta\psi$_Δt	$1.136\ 10^{-5}$	$3.406\ 10^{-5}$	$2.817\ 10^{-4}$	252	3920446
	SH_$\Delta\psi$	$2.557\ 10^{-3}$	$1.375\ 10^{-2}$	0.168		1701
10^{-4}	SH_$\Delta\psi$_Δt	$7.818\ 10^{-5}$	$2.259\ 10^{-4}$	$1.593\ 10^{-3}$	170438	194420
	ST_$\Delta\psi$	$1.331\ 10^{-3}$	$1.316\ 10^{-3}$	$1.181\ 10^{-2}$		1950
	SS_$\Delta\psi$_Δt	$8.607\ 10^{-6}$	$3.525\ 10^{-5}$	$3.899\ 10^{-4}$	154597	392041
	SH_$\Delta\psi$	$3.956\ 10^{-3}$	$1.166\ 10^{-2}$	0.125		1312
10^{-3}	SH_$\Delta\psi$_Δt	$2.320\ 10^{-4}$	$7.553\ 10^{-4}$	$7.883\ 10^{-3}$	52723	60303
	ST_$\Delta\psi$	$2.241\ 10^{-3}$	$5.702\ 10^{-3}$	$1.792\ 10^{-2}$		620
	SS_$\Delta\psi$_Δt	$6.567\ 10^{-5}$	$1.585\ 10^{-4}$	$1.453\ 10^{-3}$	9895	39110
	SH_$\Delta\psi$	$6.559\ 10^{-3}$	$1.716\ 10^{-2}$	0.119		1018
10^{-2}	SH_$\Delta\psi$_Δt	$2.224\ 10^{-3}$	$7.923\ 10^{-3}$	$7.111\ 10^{-2}$	15540	17888
	ST_$\Delta\psi$	$9.954\ 10^{-3}$	$2.630\ 10^{-2}$	$8.727\ 10^{-2}$		243
	SS_$\Delta\psi$_Δt	$8.283\ 10^{-4}$	$2.271\ 10^{-3}$	$1.478\ 10^{-2}$	862	3804

Table 3: Relative errors and number of iterations obtained for the iterative algorithm depending on different convergence criteria for TC1.

Tol.	Algorithm	L_1	L_2	L_∞	N_{param}	N_{sol}
10^{-5}	TA_T	$5.016 \; 10^{-3}$	$2.376 \; 10^{-2}$	0.269	32197	35938
	TA_S	$6.152 \; 10^{-6}$	$2.429 \; 10^{-5}$	$2.561 \; 10^{-4}$	9316700	9322946
10^{-4}	TA_T	$5.598 \; 10^{-3}$	$2.580 \; 10^{-2}$	0.284	10169	11520
	TA_S	$2.839 \; 10^{-5}$	$1.363 \; 10^{-4}$	$1.654 \; 10^{-3}$	931616	938144
10^{-3}	TA_T	$1.524 \; 10^{-2}$	$7.085 \; 10^{-2}$	0.822	3231	4032
	TA_S	$2.537 \; 10^{-4}$	$1.271 \; 10^{-3}$	$1.568 \; 10^{-2}$	93114	100898
10^{-2}	TA_T	$6.241 \; 10^{-2}$	0.274	2.459	1023	1402
	TA_S	$2.519 \; 10^{-3}$	$1.224 \; 10^{-2}$	0.142	9267	18292

Table 4: Relative errors and number of iterations obtained for the time-adaptive algorithm
depending on different convergence criteria for TC1.

Tol.	Algorithm	L_1	L_2	L_∞	N_{trunc}	N_{sol}
10^{-5}	SH_$\Delta\psi$	$6.966\ 10^{-3}$	$1.818\ 10^{-2}$	$5.878\ 10^{-2}$		573
	SH_$\Delta\psi$_Δt	$3.697.\ 10^{-4}$	$9.766\ 10^{-4}$	$3.332\ 10^{-3}$	53769	59643
	ST_$\Delta\psi$	$1.578\ 10^{-4}$	$4.254\ 10^{-4}$	$2.451\ 10^{-3}$		3503
	SS_$\Delta\psi$_Δt	-	-	-	-	n. c.
10^{-4}	SH_$\Delta\psi$	$6.966\ 10^{-3}$	$1.818\ 10^{-2}$	$5.878\ 10^{-2}$		509
	SH_$\Delta\psi$_Δt	$6.968\ 10^{-4}$	$1.979\ 10^{-3}$	$5.726\ 10^{-3}$	16557	18428
	ST_$\Delta\psi$	$5.814\ 10^{-4}$	$1.492\ 10^{-3}$	$6.711\ 10^{-3}$		1033
	SS_$\Delta\psi$_Δt	$3.279\ 10^{-6}$	$1.239\ 10^{-5}$	$8.603\ 10^{-5}$	0	2474120
10^{-3}	SH_$\Delta\psi$	$6.966\ 10^{-3}$	$1.818\ 10^{-2}$	$5.878\ 10^{-2}$		410
	SH_$\Delta\psi$_Δt	$3.699\ 10^{-3}$	$9.761\ 10^{-3}$	$3.275\ 10^{-2}$	4830	5444
	ST_$\Delta\psi$	$1.553\ 10^{-3}$	$4.226\ 10^{-3}$	$2.457\ 10^{-2}$		317
	SS_$\Delta\psi$_Δt	$2.355\ 10^{-5}$	$6.230\ 10^{-5}$	$2.341\ 10^{-4}$	0	247426
10^{-2}	SH_$\Delta\psi$	$6.892\ 10^{-3}$	$1.800\ 10^{-2}$	$5.780\ 10^{-2}$		309
	SH_$\Delta\psi$_Δt	$9.135\ 10^{-3}$	$2.409\ 10^{-2}$	$7.925\ 10^{-2}$	376	580
	ST_$\Delta\psi$	$2.756\ 10^{-3}$	$1.134\ 10^{-2}$	$7.715\ 10^{-2}$		180
	SS_$\Delta\psi$_Δt	$2.973\ 10^{-4}$	$7.884\ 10^{-4}$	$3.252\ 10^{-3}$	0	24757

Table 5: Relative errors and number of iterations obtained for the iterative algorithm depending on different convergence criteria for TC2 (n.c.: non convergence in less than 10^7 iterations).

Hydrology and
Earth System
Sciences

Discussions

Tol.	Algorithm	L_1	L_2	L_∞	N_{param}	N_{sol}
10^{-5}	**TA_T**	$1.230.\ 10^{-4}$	$4.563\ 10^{-4}$	$3.346\ 10^{-3}$	3089	3098
	TA_S	$8.741\ 10^{-6}$	$2.308\ 10^{-5}$	$7.905\ 10^{-5}$	1136193	1136199
10^{-4}	**TA_T**	$1.572\ 10^{-3}$	$4.497\ 10^{-3}$	$2.404\ 10^{-2}$	986	987
	TA_S	$2.701\ 10^{-5}$	$7.219\ 10^{-5}$	$3.095\ 10^{-4}$	113616	113616
10^{-3}	**TA_T**	$4.707\ 10^{-3}$	$1.346\ 10^{-2}$	$7.169\ 10^{-2}$	323	323
	TA_S	$1.754\ 10^{-4}$	$4.844\ 10^{-4}$	$2.391\ 10^{-3}$	11358	11358
10^{-2}	**TA_T**	$5.220\ 10^{-3}$	$1.683\ 10^{-2}$	0.101	135	135
	TA_S	$1.596\ 10^{-3}$	$4.444\ 10^{-3}$	$2.243\ 10^{-2}$	1132	1132

Table 6: Relative errors and number of iterations obtained for the time-adaptive algorithm depending on different convergence criteria for TC2.

Tol.	Algorithm	L_1	L_2	L_∞	N_{trunc}	N_{sol}
	SH_$\Delta\psi$	$9.994 \ 10^{-3}$	$1.119 \ 10^{-2}$	$1.554 \ 10^{-2}$		1644
10^{-5}	SH_$\Delta\psi$_Δt	$6.612 \ 10^{-4}$	$7.346 \ 10^{-4}$	$1.116 \ 10^{-3}$	171636	190588
	ST_$\Delta\psi$	$6.830 \ 10^{-4}$	$7.775 \ 10^{-4}$	$1.648 \ 10^{-3}$		16984
	SS_$\Delta\psi$_Δt	$7.185 \ 10^{-5}$	$7.935 \ 10^{-5}$	$1.297 \ 10^{-4}$	197481	1646346
	SH_$\Delta\psi$	$6.664 \ 10^{-3}$	$7.280 \ 10^{-3}$	$1.033 \ 10^{-2}$		1734
10^{-4}	SH_$\Delta\psi$_Δt	$3.512 \ 10^{-3}$	$3.898 \ 10^{-3}$	$5.811 \ 10^{-3}$	57312	63956
	ST_$\Delta\psi$	$1.300 \ 10^{-3}$	$1.517 \ 10^{-3}$	$2.412 \ 10^{-3}$		6504
	SS_$\Delta\psi$_Δt	$5.380 \ 10^{-5}$	$6.536 \ 10^{-5}$	$1.010 \ 10^{-4}$	41073	186351
	SH_$\Delta\psi$	-	-	-		n.c.
10^{-3}	SH_$\Delta\psi$_Δt	$2.625 \ 10^{-3}$	$2.899 \ 10^{-3}$	$4.971 \ 10^{-3}$	22047	24779
	ST_$\Delta\psi$	$4.730 \ 10^{-3}$	$5.422 \ 10^{-3}$	$1.036 \ 10^{-2}$		1297*
	SS_$\Delta\psi$_Δt	$7.569 \ 10^{-4}$	$8.820 \ 10^{-4}$	$1.402 \ 10^{-3}$	16474	31276
	SH_$\Delta\psi$	-	-	-		n.c.
10^{-2}	SH_$\Delta\psi$_Δt	$5.493 \ 10^{-3}$	$6.306 \ 10^{-3}$	$1.171 \ 10^{-3}$	7438	8812
	ST_$\Delta\psi$	$6.621 \ 10^{-3}$	$7.402 \ 10^{-3}$	$1.042 \ 10^{-2}$		810
	SS_$\Delta\psi$_Δt	$7.511 \ 10^{-3}$	$8.780 \ 10^{-3}$	$1.378 \ 10^{-2}$	5838	7535

Table 7: Relative errors and number of iterations obtained for the iterative algorithm depending on different convergence criteria for TC3 (n.c.: non convergence in less than 10^7 iterations, * convergence failed for 10^{-3}, $\tau_r = 0.90 \ 10^{-3}$).

Hydrology and
Earth System
Sciences

Discussions

Tol.	Algorithm	L_1	L_2	L_∞	N_{param}	N_{sol}
10^{-5}	TA_T	$9.814\ 10^{-3}$	$9.949\ 10^{-3}$	$1.286\ 10^{-2}$	8369	8703
	TA_S	$7.980\ 10^{-5}$	$8.797\ 10^{-5}$	$1.472\ 10^{-4}$	1357075	1357160
10^{-4}	TA_T	$1.731\ 10^{-2}$	$1.760\ 10^{-2}$	$2.748\ 10^{-2}$	2653	2934
	TA_S	$1.067\ 10^{-4}$	$1.247\ 10^{-4}$	$1.997\ 10^{-4}$	135386	135498
10^{-3}	TA_T	$2.922\ 10^{-2}$	$3.105\ 10^{-2}$	$4.545\ 10^{-2}$	889	1153
	TA_S	$1.433\ 10^{-4}$	$1.788\ 10^{-4}$	$3.367\ 10^{-4}$	13314	13397
10^{-2}	TA_T	$1.996\ 10^{-2}$	$2.449\ 10^{-2}$	$5.536\ 10^{-2}$	347	515
	TA_S	$1.851\ 10^{-3}$	$2.051\ 10^{-3}$	$3.925\ 10^{-3}$	1232	1283

Table 8: Relative errors and number of iterations obtained for the time-adaptive algorithm depending on different convergence criteria for TC3.

Hydrology and
Earth System
Sciences

Open Access

EGU

Discussions

List of Figures

Figure 1: Relative permeability as a function of the pressure for the three test cases
(L1, L2 and L3 are the three layers for test case 3).
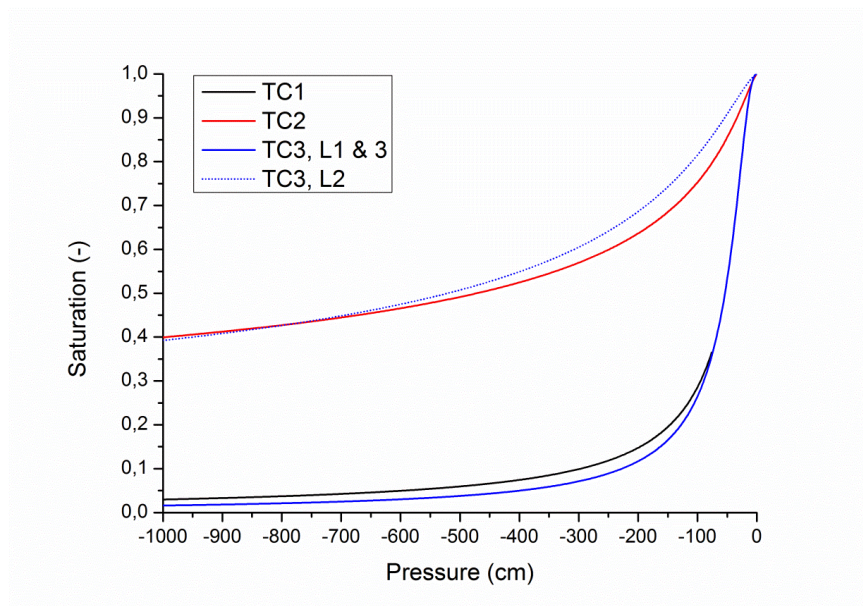
Figure 2: Water saturation as a function of the pressure for the three test cases
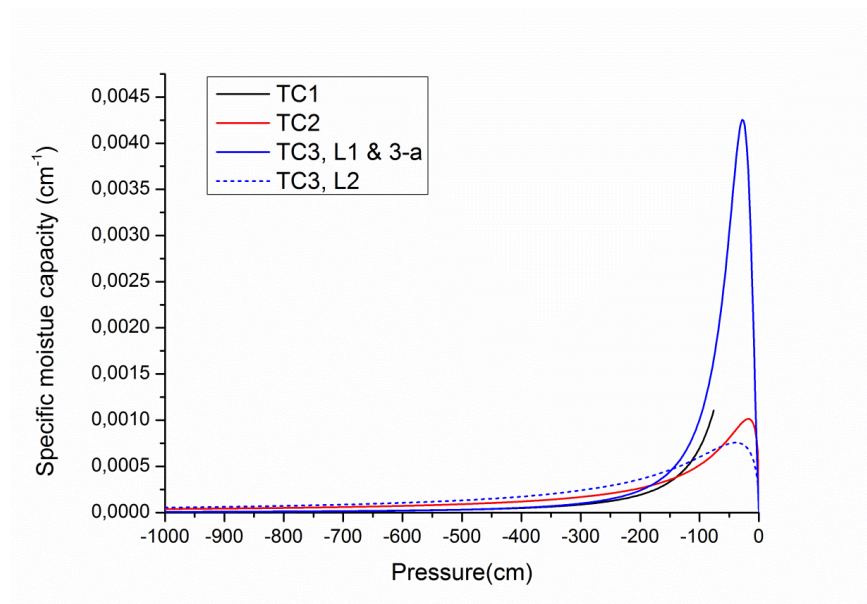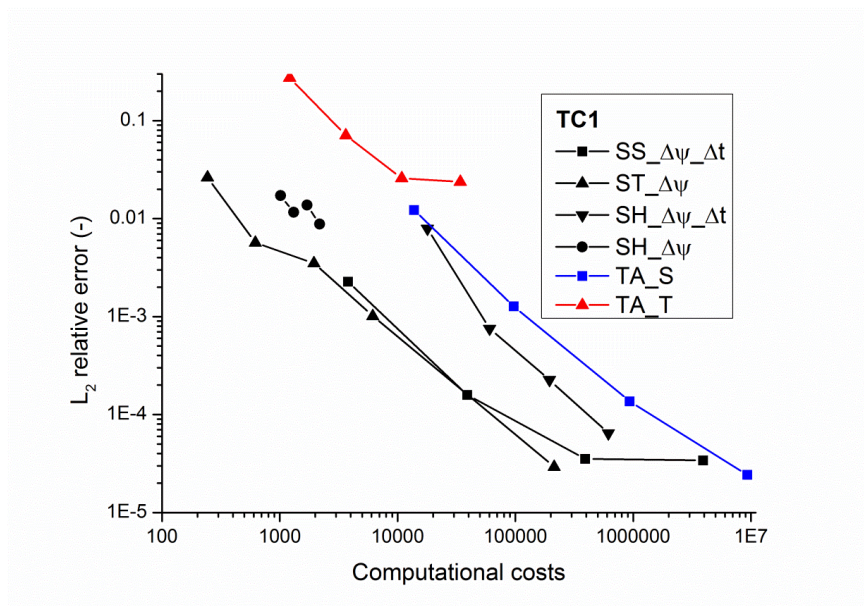(L1, L2 and L3 are the three layers for test case 3).

Figure 3: Specific moisture capacity as a function of the pressure for the three test cases
(L1, L2 and L3 are the three layers for test case 3).

Figure 4: Evolution of the L_2 relative error with computational costs for TC1.

Hydrology and
Earth System
Sciences
Discussions

Open Access

EGU
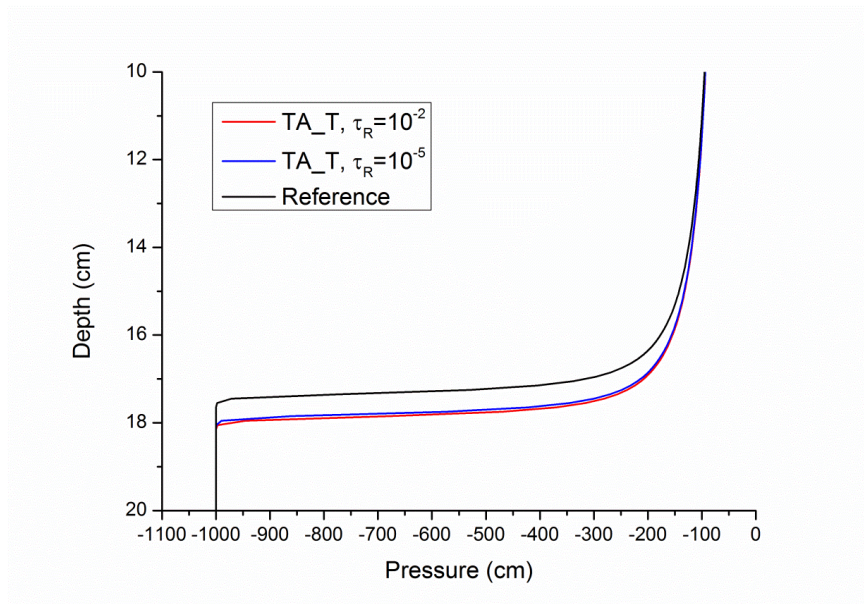
Figure 5: Pressure profiles in the domain for the TA_T algorithm.
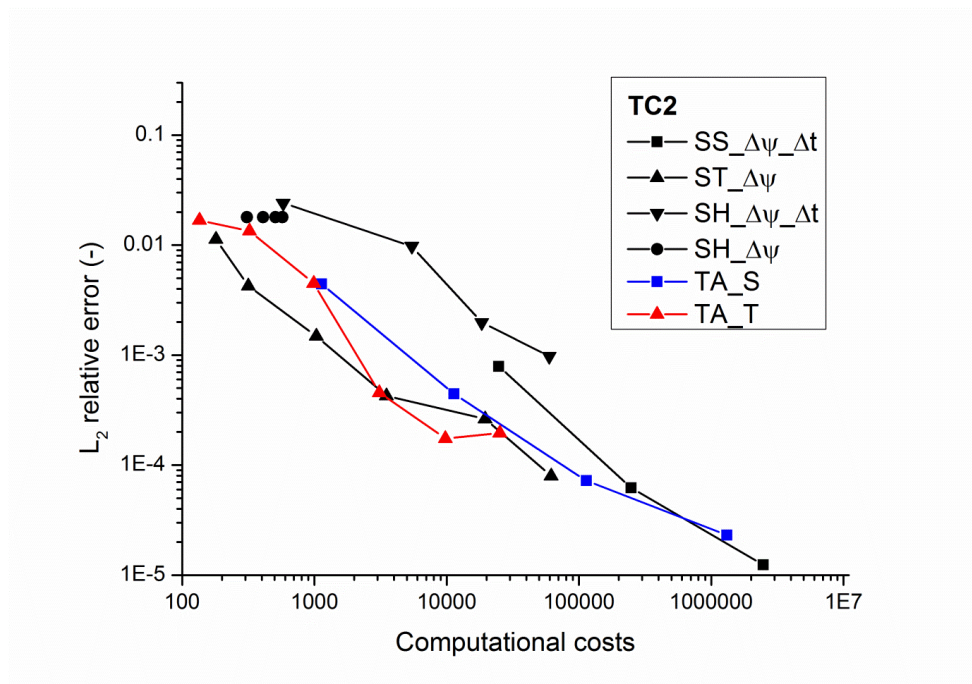
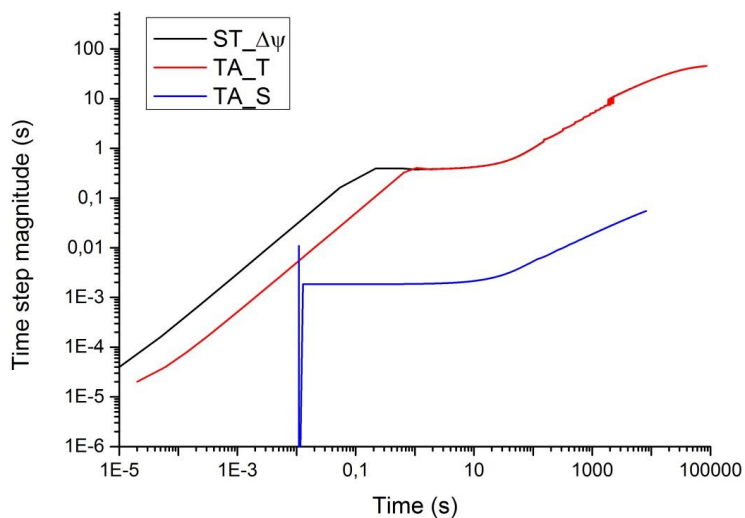Figure 6: Evolution of the L_2 relative error with computational costs for TC2.

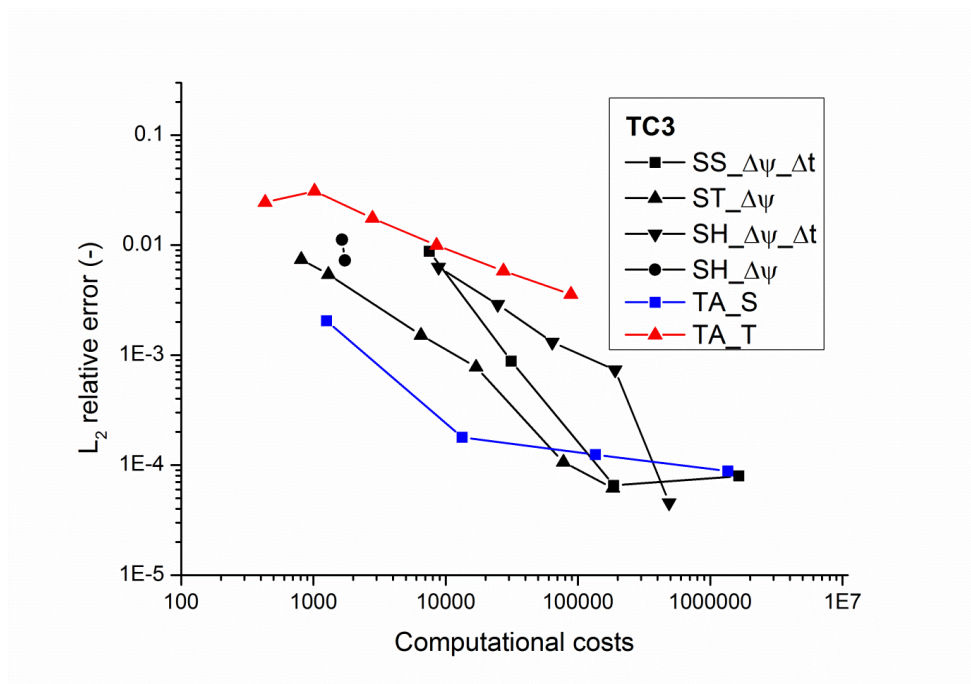Figure 7: Time step magnitudes during the simulation for TC2.

Figure 8: Evolution of the L_2 relative error with computational costs for TC3.

Hydrology and
Earth System
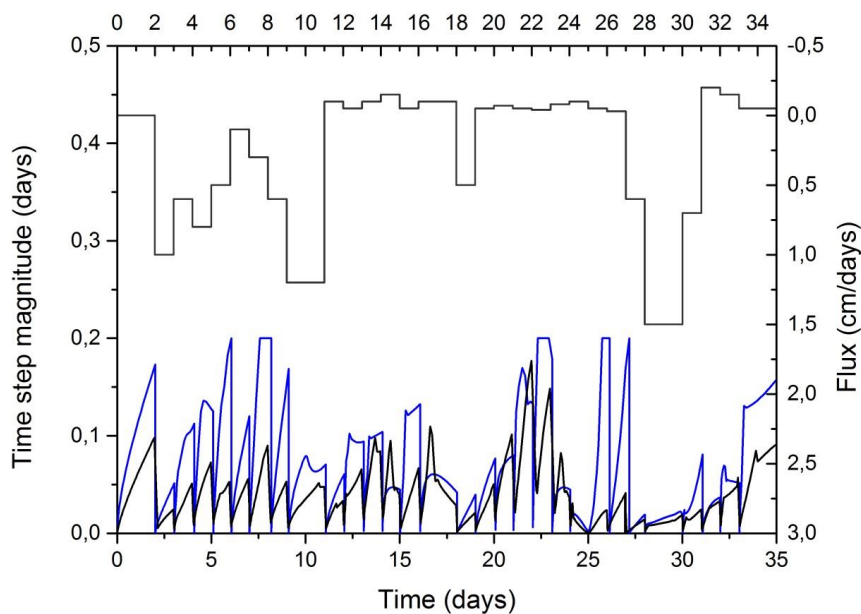Sciences
Open Access
Discussions
EGU

Figure 9: Time step magnitudes during the simulation for TC3 for the time stepping strategy based on truncation error (TA_S in blue, TA_T in black, time varying boundary conditions at the top).